

## Extending community trajectory analysis: New metrics and representation

A. Sturbois<sup>a,b,f,g,\*</sup>, M. De Cáceres<sup>c</sup>, M. Sánchez-Pinillos<sup>c,d,e</sup>, G. Schaal<sup>f</sup>, O. Gauthier<sup>f</sup>,  
P. Le Mao<sup>g</sup>, A. Ponsoero<sup>b,h</sup>, N. Desroy<sup>g</sup>

<sup>a</sup> Vivarmor Nature, 18 C rue du Sabot, 22440 Ploufragan, France

<sup>b</sup> Réserve naturelle nationale de la Baie de Saint-Brieuc, site de l'étoile, 22120 Hillion, France

<sup>c</sup> Joint Research Unit CTFC-AGROTECNIO, Crta. de St. Llorenç de Morunys a Port del Comte, km 2 25280 Solsona, Spain

<sup>d</sup> Centre for Forest Research, Department of Biological Sciences, Université du Québec à Montréal, Montreal, QC, H3C 3P8, Canada

<sup>e</sup> Faculty of Forestry and Environmental Management, University of New Brunswick, Fredericton, New Brunswick, E3B 5A3, Canada

<sup>f</sup> Laboratoire des Sciences de l'Environnement Marin, UMR CNRS 6539, Institut Universitaire Européen de la Mer, Rue Dumont d'Urville, 29280 Plouzané, France

<sup>g</sup> Ifremer, LER Bretagne Nord, CRESCO, 38 rue du Port Blanc, 35800 Dinard, France

<sup>h</sup> Saint-Brieuc Agglomération Baie d'Armor, 5 rue du 71ème RI, 22000 Saint-Brieuc, France

### ARTICLE INFO

#### Keywords:

Ecological variability  
Impact assessment  
Initial state  
Community dynamics  
Trajectory analysis  
Representation tools

### ABSTRACT

Ecological research focuses on the spatio-temporal patterns of ecosystems and communities. The recently proposed framework of Community Trajectory Analysis considers community dynamics as trajectories in a chosen space of community resemblance and utilizes geometrical properties of trajectories to compare and analyse temporal changes. Here, we extend the initial framework, which focused on consecutive trajectory segments, by considering additional metrics with respect to initial or baseline states. Addressing questions about community dynamics and more generally temporal and spatial ecological variability requires synthetic and efficient modes of representation. Hence, we propose a set of innovative maps, charts and trajectory roses to represent trajectory properties and complement the panel of traditional modes of representation used in community ecology. We use four case studies to highlight the complementarity and the ability of the new metrics and innovative figures to illustrate ecological trajectories and to facilitate their interpretation. Finally, we encourage ecologists skilled in multivariate analysis to integrate CTA into their toolbox in order to quantitatively evaluate spatio-temporal changes.

### 1. Introduction

Ecology aims to identify processes underlying the distribution and abundance of organisms, along with those that determine how organisms modify their abiotic environment (Kendall, 2015). Two paradigms are widely accepted amongst ecologists: (1) biological assemblages are amongst the best response variable to estimate the impact of changes in natural ecosystems and (2) temporal changes in community assemblages indicate that some processes have been at work to generate them (Legendre and Gauthier, 2014). Temporal changes in biological assemblages are the sum of local colonisation and extinction events, as well as changes in the biomass and relative abundance of taxa within and amongst samples (Buckley et al., 2018). Quantifying and forecasting temporal changes in biodiversity and ecological shifts due to both natural and anthropogenic drivers is therefore a central issue in ecology (Dornelas et al., 2013). This requires repeatedly sampling target

communities over time and, often, studying their evolution compared to an initial state and/or a chosen baseline (goal defined as an ecological state to be achieved (Bioret et al., 2009)). To this aim, consecutive ecological states are defined by a set of environmental or biological parameters used as descriptors of the ecosystem existing on a given location, at a given time (chemical and physical parameters, absolute or relative abundance of population species, specific richness, pollution level...). In a period of dramatic increase of anthropogenic impacts, such approaches are particularly relevant for studying natural variability, and have potential implications in management and ecological restoration or in the development of ecological indicators.

The development of community ecology has historically been influenced by static depictions of inherently dynamic processes which led to many important insights about the structure of communities (Yang, 2020). Analytical and representation methods of biodiversity changes over time constitute an essential and important domain of innovation

\* Corresponding author.

E-mail address: [anthony.sturbois@espaces-naturels.fr](mailto:anthony.sturbois@espaces-naturels.fr) (A. Sturbois).

<https://doi.org/10.1016/j.ecolmodel.2020.109400>

Received 28 July 2020; Received in revised form 13 December 2020; Accepted 14 December 2020

Available online 24 December 2020

0304-3800/© 2020 Elsevier B.V. All rights reserved.

(Cimon and Cusson, 2018; Magurran et al., 2019) to study dynamics of natural systems since the beginning of community ecology (Elton, 1927). Accordingly, Yang (2020) suggests specific and complementary ways to continue building towards a more temporally explicit framework for community ecology, notably, by increasing the representation of temporal changes and developing specific and general insights into event- or factor- driven dynamics. In this way, complementary metrics are needed to document community and environmental changes (Cimon and Cusson, 2018). While the availability of long-term, large-scale, and high-resolution data is the most limiting factor to study temporal patterns in biodiversity (Dornelas et al., 2013), the development of methodological approaches to analyse, synthesize, and ultimately represent the dynamics of ecological systems is also an essential issue.

Until now, most analytical and representation frameworks have been based on the comparison of synchronous observations across sites and between repeated surveys (M. De Cáceres et al., 2019). One common approach is to analyse independently the changes observed between two surveys and to repeat this step as many times as necessary to cover the corresponding study period. However, this type of procedure quickly becomes inefficient as the number of samples increases. A potential solution to deal with long-term data sets could be to discard intermediate surveys and to focus only on starting and ending time points of a study period. However, this may hide crucial changes occurring during intermediate periods (i.e. transitional states) and, hence its usefulness to study the dynamics of ecological systems may be limited.

Multivariate analyses have been widely adopted for many decades in ecology, embracing all forms of statistical analyses applied to data in which more than one character are observed per individual (Kendall, 1958). Several multivariate statistical frameworks focus on testing hypotheses of community dynamics (Buckley et al., 2018). Consequently, multivariate frameworks still constitute the primary approach to analyse ecological datasets and an important source of methodological innovations. A common approach is the calculation of dissimilarity indices, which allows differences between a pair of ecological states to be summarized in a single metric. Since community data tables can represent both temporal and spatial variation of ecological states, the resulting symmetric dissimilarity matrices can contain spatial, temporal or spatio-temporal information. Then, the use of ecological trajectories in a multivariate space defined by the calculation of a dissimilarity index between all pairs of observations allows to representing the dynamics of a system. Ordination methods are therefore often complemented with trajectory analyses, in which changes over time or as a response to natural or anthropogenic pressures are represented by a set of vectors linking consecutive ecological states. These approaches have been previously applied to a wide variety of ecological systems, including plant assemblages (Austin, 1977; Fukami et al., 2005), bird assemblages (Hudson and Bouwman, 2007; Sica et al., 2018; Haig et al., 2019), and aquatic (Matthews et al., 2013; Mathers et al., 2016; Boit and Spencer, 2019; David et al., 2020) or marine ecosystems (Dauvin and Ibanez, 1987; Smith et al., 2010; Legendre and Salvat, 2015; Cimon and Cusson, 2018). In this context, geometric properties of trajectories, defined in the space of an ordination diagram, constitute relevant parameters to study the dynamics of ecological systems, including intermediate transitional states. The geometric study of community trajectories has sometimes been defined by two or three axes of an ordination space (Boit and Spencer, 2019; Matthews et al., 2013) but this has the drawback of discarding the information contained in additional dimensions. In order to generalize this approach, M. De Cáceres et al. (2019) considered community dynamics as trajectories in a chosen space of community resemblance, with no limit in the number of dimensions included. In the Community Trajectory Analysis (CTA) framework, trajectories are considered as objects composed of trajectory segments to be analysed and compared using their metrics based on their geometry in a multivariate space.

In 2D multivariate ordinations, accounting for fine-scale variability

hinders readability especially when the number of sites and/or surveys is high, even if different line formats and colours are used to facilitate the identification of different trajectories. A common approach to represent the amount of change across space between two surveys ( $t_1$  and  $t_2$ ) is to produce a single map (i.e. a plot on geographical axes) in which, for instance, the symbol size is proportional to the distance between states ( $x_1$  and  $x_2$  for each sampling unit) (Bacouillard et al., 2020; Kröncke et al., 2011). However, with this method, the addition of one more survey involves the production of two more maps to represent changes between  $t_2$  and  $t_3$  states and the overall change between  $t_1$  and  $t_3$  after the last survey. For three ecological surveys, this method is still doable, but it fails to represent simultaneously all ecological trajectory segments and, more importantly, information about ecological directions. Although mapping diversity or similarity indices are fused in many ecological studies (Granger et al., 2015), mapping temporal changes through symbols representing trajectory metrics, rather than the dissimilarity between consecutive surveys, has not yet been sufficiently explored in our opinion. Considering the direction of ecosystem dynamics, circular statistics (analysis of directions ranging from 0 to 360° (Batschelet, 1981)), which are commonly used in behavioural ecology, appear as promising alternatives to quantitatively represent the direction of dynamics of ecological systems, and to complement traditional modes of representation. In this perspective, circular statistics may offer significant insights to represent trajectory properties, that are not evident from qualitative comparisons of ordination diagrams, as suggested for food webs by Schmidt et al. (2007).

In this paper, we propose an extension of the CTA framework to represent temporal changes between more than two temporal surveys with respect to a chosen baseline state. As initially defined in M. De Cáceres et al. (2019), CTA was focused on the study of ecological states corresponding to consecutive surveys. A complementary overarching question being to know how ecological states change with respect to an initial state and/or to a baseline, an alternative way to analyse trajectories can be developed, considering these fixed ecological states as central in the analysis. As CTA allows calculating lengths, angles between trajectory segments and directionality of trajectories, it is likely to be a complementary framework to approaches comparing data to initial state based on distances or distance sequences (Bacouillard et al., 2020; Bagchi et al., 2017; Legendre, 2019; Legendre and Salvat, 2015), differences in cluster classification (Kröncke et al., 2011) or shifts along multivariate axes (McLean et al., 2019).

The main contributions of this article concern: (1) the extension of CTA with new metrics that describe community trajectories with respect to a chosen state and new ways of defining angles, (2) the synthetic representation of trajectories through three innovative figure concepts: (a) map of changes between ecological states including information about recovering and departing dynamics with respect to a baseline or initial state, (b) a chart of trajectories from initial state to represent trajectory paths and overall changes, (c) trajectory rose to summarise, in a circular framework, the direction and length of ecological trajectories. Four case studies are then developed to illustrate the use of our proposed metrics and representation tools. Finally, their potential applications and limitations are discussed.

## 2. Methods

The methods detailed in the following subsections are based on trigonometrical properties of trajectories in  $n$ -dimensional spaces and their representation in innovative synthetic figures.

### 2.1. Characterizing ecological trajectories

#### 2.1.1. CTA framework

We follow here the terminology of De Cáceres et al. (2019), for describing and comparing community trajectories in a multidimensional space. Given a target community whose dynamics are surveyed, let  $o_i$ ,

$o_2, \dots, o_n$  be an ordered set of  $n$  observations ( $n > 1$ ) and  $t_1, t_2, \dots, t_n$  the corresponding set of ordered survey times (i.e.  $t_1 < t_2 < \dots < t_n$ ) (Fig. 1, A). For all  $i$  in  $\{1, 2, \dots, n\}$ ,  $x_i$  contains the coordinates, or ecological state, corresponding to  $o_i$  in a multidimensional space  $\Omega$ . The geometry of the trajectory  $T$  is formalized using a set of  $n - 1$  directed segments  $\{s_1, \dots, s_{n-1}\}$ , where  $s_i = \{x_i, x_{i+1}\}$  is a segment with endpoints (community states)  $x_i$  and  $x_{i+1}$  (Fig. 1, A).

The multivariate space  $\Omega$  supporting CTA is defined by the choice of dissimilarity coefficients (e.g. Bray-Curtis), which is used to evaluate resemblance between pairs of community observations (Legendre and De Cáceres, 2013; M. De Cáceres et al., 2019). Note that users can choose the scale of CTA by setting the scale at which communities are defined. For example, community trajectories may be studied at the site level, or

at larger scales (e.g. landscape or regional level) if community data are aggregated across sites.

2.1.2. Trajectory metrics

Original CTA metrics relevant for this paper are first introduced (Section 2.1.2.1) and new contributions are detailed from Section 2.1.2.2.

2.1.2.1. Original CTA metrics. The trajectory segment length is the distance between two consecutive ecological states (De Cáceres et al., 2019). The greater the length of a trajectory segment, the greater the distance between ecological states is. The length of a segment  $s_i$  is given by the distance between its two endpoints in space  $\Omega$  (Fig. 1, A):  $L(s_i) = d$

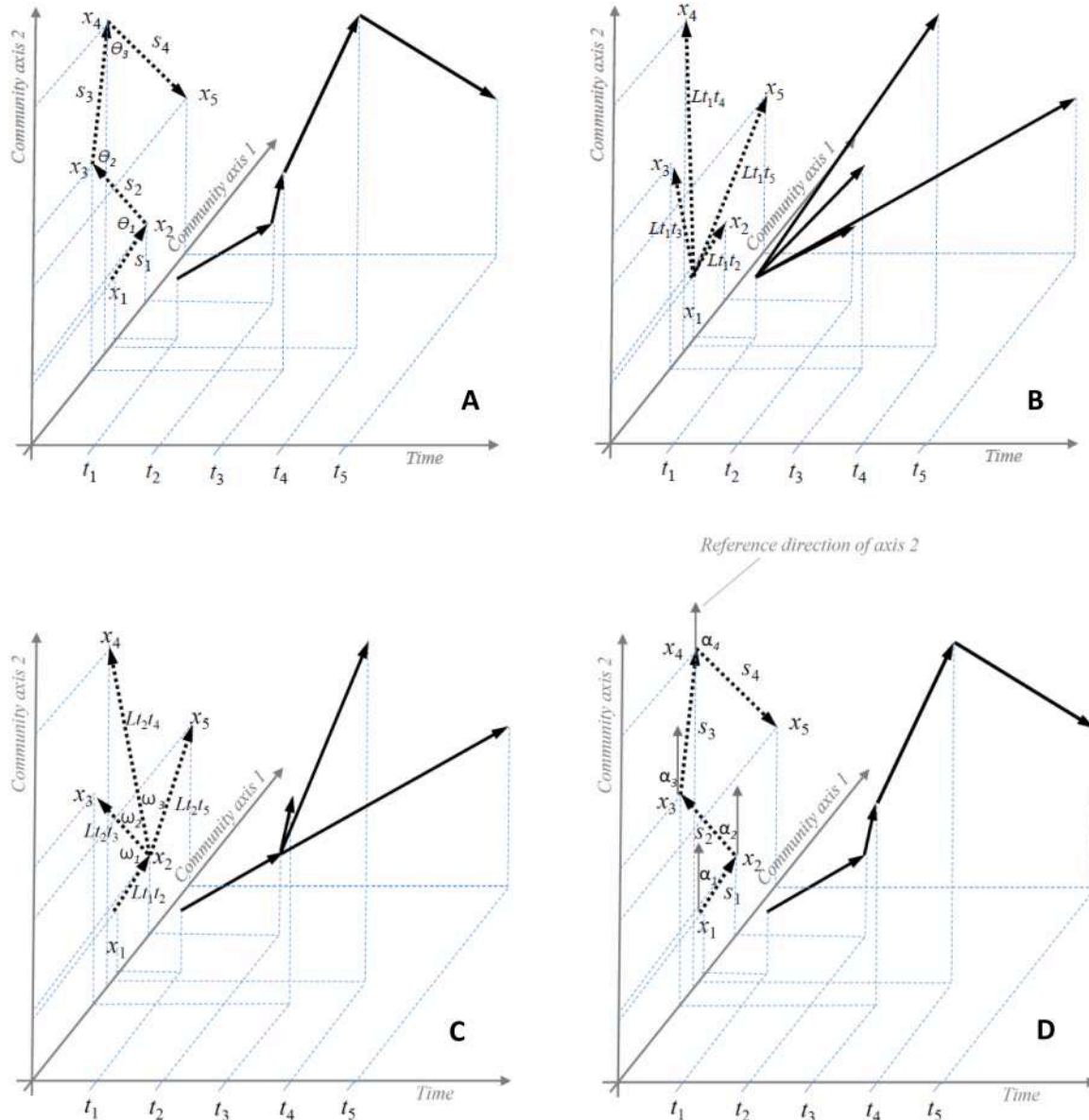


Fig. 1. Example of an ecological state trajectory  $T$  from five observations ( $o_1, \dots, o_5$ ) at five ordered points in time ( $t_1, \dots, t_5$ ). Ecological state observations are represented using a corresponding set of states ( $x_1, \dots, x_5$ ) in a multidimensional space (two principal axes are shown only). The trajectory is represented on the plane formed by community axes and in a three dimensional plot including the time axis (continuous arrows). The trajectory can be also formalized in terms of four directed consecutive segments ( $s_1, \dots, s_4$ ) in the same space (A).  $x_i$  represents positions (coordinates) and  $s_i$  are segments, so that the sum of consecutive segment lengths is the total length of the trajectory pathway. One can also consider vectors with respect to the initial state (B,C) with four vectors departing from  $x_1$  ( $x_1x_2, \dots, x_1x_5$ ). Lengths  $Lt_1t_i$  measure the net change between  $t_1$  and  $t_i$  (B). Several spherical angles ( $\angle$ ) can be considered, with different interpretation:  $\angle \Theta$  ( $x_i, x_j, x_k$ ) is calculated between consecutive segments and defined as the change in direction of vector  $x_j-x_k$  with respect to vector  $x_i-x_j$  in this plane (A);  $\angle \omega$  ( $x_1, x_i, x_j$ ) is calculated with respect to the initial state and defined as the change in direction of vector  $x_i-x_j$  with respect to vector  $x_1-x_i$  in this plane(C);  $\angle \alpha$  is calculated between each trajectory segment and a chosen direction (here axis 2) in a 2D multivariate space (D).

$(x_i, x_{i+1})$ . The *trajectory path length* (De Cáceres et al., 2019) is the total length of all site trajectory segments over surveys of a study period. This metric contributes to informing about the overall temporal variation of the state of a site within a study period:

$$L(T) = \sum_{i=1}^{n-1} L(s_i) = \sum_{i=1}^{n-1} d(x_i, x_{i+1})$$

Lengths of segments (or subtrajectories) are influenced by the time interval between surveys. Hence, lengths alone do not allow proper consideration of ecological dynamics (i.e. the speed of change). To this aim, a better alternative is to consider *trajectory speeds*, after dividing lengths by the time interval between observations  $S(s_i) = L(s_i) / (t_{i+1} - t_i)$ .

Another aspect of community dynamics is approached by the calculation of *angles* (De Cáceres et al., 2019). Let  $\{x_i, x_j, x_k\}$  be a triplet of ecological states of a trajectory  $T$  that are ordered in time (i.e. where  $t_i < t_j < t_k$ ). If the set of distances  $\{d(x_i, x_j), d(x_i, x_k), d(x_j, x_k)\}$  fulfills the triangle inequality, then angles can be measured on the Euclidean plane that contains these three states (Fig. 1, A). The angle  $0 \leq \Theta(x_i, x_j, x_k) \leq 180^\circ$  is defined as the change in direction of vector  $x_j - x_i$  with respect to vector  $x_k - x_i$  in this plane. The trajectory is linear when  $\Theta_i = 0^\circ$ . If  $\Theta_i = 180^\circ$ , trajectory is still linear but opposite in sense.

Finally, the overall *directionality* of trajectories provides information about the consistency with which the site is following the same direction and, therefore, the stability of the drivers of ecological dynamics that condition ecological states. The directionality statistic (De Cáceres et al., 2019) of a trajectory is measured using the following:

$$DIR(T) = \frac{\sum W_{ijk} * \left( \frac{180 - \theta_{ijk}}{180} \right)}{\sum W_{ijk}}$$

where  $\Theta_{ijk} = \Theta(x_i, x_j, x_k)$ ,  $w_{ijk} = d(x_i, x_j) + d(x_j, x_k)$  and summation is over all  $r$  time-ordered triplets.  $DIR(T)$  is bounded between 0 and 1 where the maximum value corresponds to a straight trajectory. This metric is useful to distinguish between communities subjected to stabilizing (non-directional) selection from those influenced by directional or disruptive selections (Lamothe et al., 2019; Matthews et al., 2013).

**2.1.2.2. Trajectory analysis with respect to an initial state. Net change ( $L_{t_1-t_j}$ )** - Let  $x_1$  be an initial (or baseline) state. The *net change* is defined for any pair of states  $\{x_1, x_j\}$  as the length (i.e. distance)  $L_{t_1-t_j} = d(x_1, x_j)$  between  $x_1$  and  $x_j$  (Fig. 1, B). When calculated at the scale of an overall study period between  $x_1$  and  $x_{n \text{ survey}}$ , this metric evaluates the difference between the community at the end of the study period and its initial state (*overall net trajectory change*).

**Net change ratio (NCR)** - The net change ratio is defined as the ratio between the overall net trajectory change and the trajectory path length:  $NCR = L_{t_1-t_{n \text{ survey}}} / L(T)$ . NCR informs about the straightness of recovering or departing processes with respect to the initial state.

A high NCR indicates that a great part of the trajectory path contributes to net changes and illustrate a relative stability of drivers of ecological dynamics. Inversely, a low NCR coupled with high segment lengths illustrates instability of drivers of ecological dynamics and highlights that a small part of the trajectory path contributes to net changes. In this sense, NCR and  $DIR(T)$  are complementary metrics. High  $DIR(T)$  would be equal to High NCR but, a low  $DIR(T)$  may not be equal to low NCR depending on segment lengths.

**Recovering or Departing Trajectory (RT)** - Let us now consider a  $\{x_1, x_j, x_k\}$  triplet where the first element corresponds to the baseline state ( $t_1 < t_j < t_k$ ). The net change of the  $\{x_1, x_j\}$  pair,  $L_{t_1-t_j} = d(x_1, x_j)$ , and the net change of the  $\{x_1, x_k\}$  pair,  $L_{t_1-t_k} = d(x_1, x_k)$ , can be used to qualify the

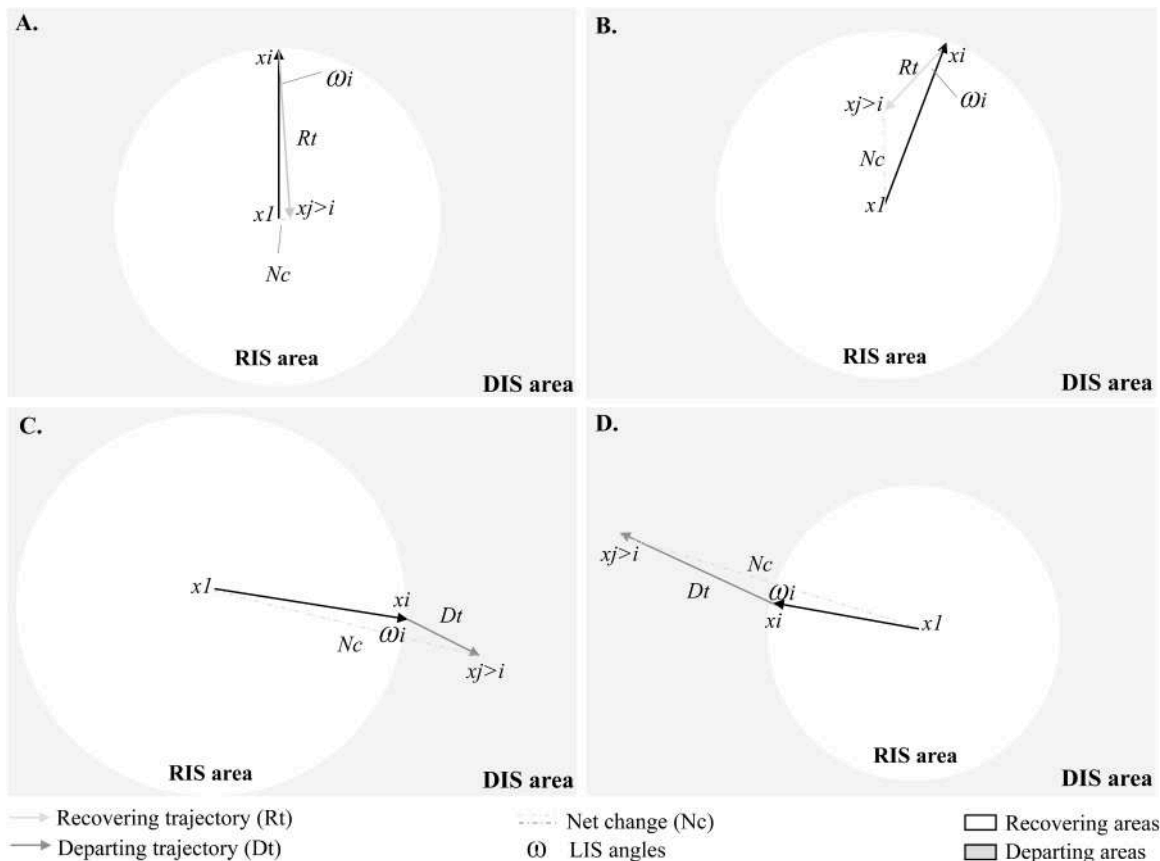


**Fig. 2.** Different *scenarii* (A, B, C and D) of lengths and  $\omega$  induce recovering (Rt) or departing (Dt) trajectories from  $x_1$ . In a 2D multivariate space, the recovering area (RIS, white) is conceptually defined by a circle with centre  $x_1$  and diameter  $2 L_{t_1, t_i}$ , the rest of the space being considered as the departing area (DIS, grey). Angles (LIS) and lengths both contribute to net changes. Only two dimensions are shown. In a n-dimensional space, RIS area become an hyper-sphere.

dynamics with respect to the initial state as *recovering* (i.e. return to the initial state) or *departing* (i.e. increasing distance from the initial state). Let us define *RDT* (*Recovering or Departing Trajectory*) metric as the difference between these two distances:  $RDT = d(x_i, x_j) - d(x_i, x_k)$ .  $RDT > 0$  indicates a closer ecological state in  $x_k$  than in  $x_j$  and, consequently, implies a recovering towards the initial state (*RIS*)  $x_i$  between  $x_j$  and  $x_k$  (Fig. 2). Inversely,  $RDT < 0$  indicates a farther ecological state in  $x_k$  than in  $x_j$  and consequently implies a departure from the initial state (*DIS*) between  $x_j$  and  $x_k$ . *RDT* could help to determine the effectiveness of management on the ecological state of a community with respect to a baseline state defined as an objective to be achieved or inversely the impact of a natural or anthropogenic event. Additionally, in a context of disturbances in which  $x_i$ ,  $x_j$ , and  $x_k$  represent pre-disturbance, disturbed, and post-disturbance states, respectively, *RDT* can be used as a measure of the ecosystem resilience.

**2.1.2.3. Linearity of changes with respect to an initial state. Linearity with respect to the initial state ( $\omega$ )** - We propose to calculate the angle  $\omega$  ( $x_i, x_j, x_k$ ) between trajectory vectors  $\{x_i, x_j\}$  and  $\{x_j, x_k\}$  in a 0–180° system considering 0° as the same direction of the first vector (Fig. 1, C). Angles allow assessing the *linearity of changes with respect to an initial state* (*LIS*) according to a vector of reference [i.e. first segment or subtrajectory (aggregation of segments) of an ecological trajectory] in the Euclidean space. When space  $\Omega$  is 2D,  $\omega$  (as well as  $\Theta$ ) can be reported in a 0–360° system, if desired (see examples in Fig. 10 and 13).

The direction (angles) within a trajectory constitutes an important component of the ecological variability, as different directions do not make the same ecological sense, even if the lengths (or speeds) of these trajectories are equivalent. There is a correspondence between  $\omega_i$  angles and *RDT*: Indeed, if angle  $\omega_i < 90^\circ$  or  $\omega_i > 270^\circ$  the trajectory departs from the  $x_i$  initial state (i.e.  $RDT < 0$ ) regardless of trajectory length. On the contrary, if  $90^\circ < \omega_i < 270^\circ$  the trajectory recovers (*RIS* area;  $RDT > 0$ ) or departs (*DIS* area;  $RDT < 0$ ) depending on both angle and length values (Fig. 2).

**2.1.2.4. Directions with respect to the plane formed by two axes.** If users decide that the variance is sufficiently explained by the first two axes of an ordination, it becomes relevant to consider all trajectory segment directions with respect to the interpretation of axes, normally done using the loadings of original variables or their degree of correlation with additional variables.

**Segment directions in 2D ordination ( $\alpha$ )** - We propose to assess angles  $\alpha$  ( $x_i, x_j$ , axis 2) considering the second axis of the ordination diagram as the North (0°) (Fig. 1, D).  $\alpha$  allows comparing segment direction with respect to the influence of the variables used to interpret the two ordination axes.

**2.1.2.5. Testing and comparing trajectory directions.** Circular data need special treatment in data analysis: an angle of 355° is much similar to an angle of 5° than it is to an angle of 330°, hence a simple arithmetic mean for example can be quite misleading (Landler et al., 2018). In order to analyse the uniformity of directions, Landler et al. (2018) recommended using the Rayleigh test when unimodal departure from uniformity is expected, and the Hermans-Rasson test (HR) for multimodal departures (Landler et al., 2019). Such tests allow verifying if there is a unimodal bias in the distribution of angles directions, i.e. if the direction of vector  $x_j - x_k$  changes with respect to vector  $x_i - x_j$  are evenly distributed (null hypothesis) or concentrated around one or more particular directions. One should prioritize the Rayleigh or the HR tests- depending the type of distribution of direction and following Landler et al. (2019) recommendations. The Watson-William's two test is used to test the homogeneity (null hypothesis) or the significance of difference of segment direction between different factors.

### 2.1.3. Software

To facilitate conducting the extension of the CTA framework, function options and new functions have been developed to calculate metrics considering  $x_i$  as a constant baseline over time. This new set of CTA tools has been integrated into a new version (v.1.7.9) of the package 'vegclust' (De Cáceres et al., 2010) available on CRAN and GitHub repositories.

## 2.2. Representing the variability of ecological states and trajectories

### 2.2.1. Mapping trajectory dynamics with respect to an initial state

Here we suggest the use of maps to represent site scale dynamics through geometrical properties of trajectories in synthetic figures accounting for temporal variability at the sampling unit scale.

In order to avoid multiple distance maps between every pair of surveys, we propose the use of a single map to represent all at once for each site of a study area: (1) net change between  $x_i$  and  $x_{n-survey}$ , (2) segment length (or subtrajectory length,  $S_{i>1}$ , and  $S_{j>i}$ ) and (3) *RIS* or *DIS* segment or subtrajectory lengths between  $x_i$  and  $x_{n-survey}$ .

Symbols proposed in our synthetic map to represent net change and intermediate segments or subtrajectories (defined arbitrarily if  $n-survey > 3$ ) are detailed in Fig. 3. Net changes are represented through a circular symbol proportional to the length to vector  $x_i - x_{j>i}$ . On both sides, a bottom triangle symbol represents the  $x_i - x_{j>i}$  vector and a top triangle the  $x_{i>1} - x_{j>i}$  vector. For both triangles, the size is proportional to the length of respective vectors, while the orientation and colour of the top triangle illustrate the direction (recovering or departing) of the second vector with respect to the initial or baseline state. When more than three ecological states are used, directionality of subtrajectories can be represented with colors in both triangles (Fig. 4).

In this map, circles representing net changes are drawn on the geographical coordinates of sampling locations, while the bottom and top triangles are placed on the map by subtracting or adding an arbitrary value to the Y coordinate.

It may be relevant to define subtrajectories according to a critical event, which influence ecological states [e.g. new pressures, management activities, disturbance (fire, storm, volcanic eruption, oil spill...)] or to a period considered as a baseline in order to help to better understand the shape of trajectories in terms of lengths and angles before and after perturbation. In this case, one should adapt the temporal period represented in the bottom triangle. Inversely, without a *a priori* knowledge about such event, the occurrence of saltatory and non-directional trajectories (Lamothe et al., 2019; Matthews et al., 2013), which vary with the overall shape of the trajectory path could help to identify key periods in the history of an ecosystem regarding environmental or other contextual parameters.

### 2.2.2. Adding CTA metrics to ordination diagrams

Trajectories are traditionally represented on 2D or 3D ordination diagrams using arrows for segments. Here, we propose to complete this kind of chart by adding information about trajectory metrics such as net changes. Data point symbols represent the coordinates of each ecological state according to the axes of the ordination diagram and lines represent segments between transitional ecological states. The novelty lies in representing the distance to the initial state (i.e. first state of the time series) and time by the dot size and colour, respectively. If a single trajectory is represented and one wants to better illustrate the evolution of net changes over time, the trajectory can be centred around the initial state by subtracting the coordinates of the state corresponding to the initial state ( $x_i$ ) from the coordinates of all ecological states.

### 2.2.3. Trajectory rose diagrams

We propose to use a Trajectory Rose (TR) to represent the distribution of directions in the multivariate space  $\Omega$ , as it is traditionally done in meteorology to represent wind directions and speeds (Azorin-Molina et al., 2017; Cieszyńska and Stramska, 2018) or in currentology (Dalbosco et al., 2020; Dufresne et al., 2014). The TR consists of a circular

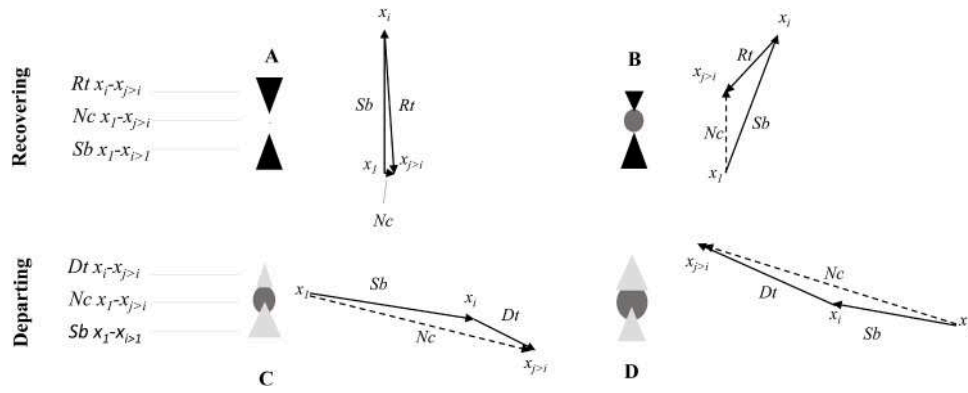


**Fig. 3.** Symbols used to represent site ecological net change between ecological state  $x_1$  and  $x_{j>i}$  (circle) and segment or subtrajectories for  $Sb x_1-x_{j>i}$  and  $Rt x_{j>i}$  or  $Dt x_{j>i}$  (triangle): the size of the symbols corresponds to the length of segments. Recovering segment or subtrajectories ( $Rt x_{j>i}$ ) are represented with black triangles in A and B whereas departing ( $Dt x_{j>i}$ ) appears in grey ones (C and D). Trajectory *scenarii* come from Fig. 2.

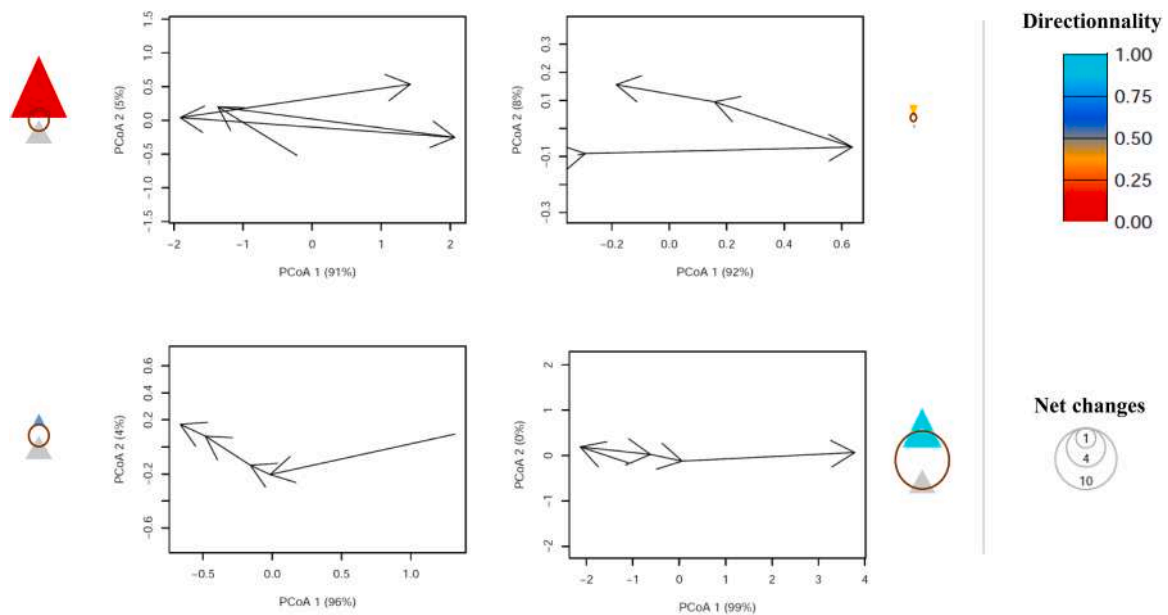


**Fig. 4.** Examples of RIS, DIS illustrating temporal ecological variability. The size of brown circles is proportional to the net change between  $x_1$  and  $x_5$ . Grey bottom triangles represent the first segment between  $x_1$  and  $x_2$  used as a reference, and the top triangle represents the mean length of the following segments ( $x_3$  to  $x_5$ ) respectively orientated and coloured according to RIS/DIS trajectory and directionality.

bar plot of angles ranging from  $0\hat{A}^\circ$  to  $360\hat{A}^\circ$ . The barplot structure of TR allows representing factors in different bar sections. Depending on the aim of the analysis, users can choose to represent  $\Theta$ ,  $\omega$  or  $\alpha$  angles in a TR.

**2.2.3.1. Distribution of  $\Theta$ ,  $\omega$  values.** The baseline state TR provides a synthetic visualisation of ecological trends at the scale of a study area according to directional changes ( $0-360^\circ$ ) of one vector with respect to the previous one for each consecutive triplet over time. Users can choose to represent distributions of  $\Theta$ , or  $\omega$ , angles in order to analyse changes of direction of each triplet or the direction of each segment with respect to the previous or the first segment of the trajectory, respectively.

Angles  $\Theta_i$  between segments  $x_i-x_{j>i}$  and  $x_{j>i}-x_{k>j}$  are defined between  $0^\circ$  and  $180^\circ$  when considering all multivariate dimensions, or can be reported in a  $0-360^\circ$  system if calculated from 2D coordinates. Angles  $\omega_i$  between segments  $x_1-x_{i>1}$  and  $x_{i>1}-x_{j>i}$  are also reported in a  $0-360^\circ$  system when calculated on 2D coordinates. At this step of the procedure, the user must consider whether the variance explained by the two first components is high enough to evaluate angles in a  $0-360^\circ$  system.

A value of  $0^\circ$  indicates a straight DIS segment with no change of

direction with respect to  $x_1-x_{i>1}$  vector. The distribution of angles is represented in barplots whose size indicates the number of segments following a given direction: *RIS* on the bottom part ( $90^\circ < \omega_{RIS} < 270^\circ$ ) and *DIS* in both parts depending on the length of the second segment of each triplet. Lengths of vector  $\{x_j, x_k\}$  are aggregated on the top of each bar section and coloured according to distance, in order to underline if direction trends occur in short or long trajectories.

**2.2.3.2. Distribution of  $\alpha$  values.**  $\alpha$  angles are calculated considering the second axis of the ordination diagram as the North ( $0^\circ$ ) and represented in a TR in order to illustrate distribution of segment direction in a 2D Euclidean space. It allows the characterization of the nature of change by comparing segment direction with respect to the interpretation of ordination axes. Variables names aiding the interpretation of directions can be positioned in the periphery of the TR (see Fig. 10).

**3. Ecological applications**

Four ecological applications were chosen to illustrate the proposed CTA metrics and modes of representation in different ecological systems.

### 3.1. Ecological application 1 – Temporal variability of waterbird communities in a marine protected area

The national nature reserve of Saint-Brieuc (Brittany, France) is a marine protected area designed in 1998 to protect wintering birds. Anatidae populations are monitored each winter as part of the International Waterbird Census (IWC). CTA has been performed on the nine most abundant species for which a census has been performed during 21 wintering, from 2000 to 2020 (Supplementary data - Appendix A). Anatidae monitoring has been carried out each year in January and encompassed the overall presumed functional area (i.e. intertidal feeding ground). Lengths, angles, and directionality were calculated (Supplementary data - Appendix B). The temporal variability of the bird community was illustrated with an ordination diagram centred on the initial survey and representing time and net change using symbol colour and size, as suggested in SubSection 2.2.2. For the trajectory rose, a bar plot of  $\Theta$  angles of each consecutive triplet ranging from  $0^\circ$  to  $360^\circ$  was produced (range of  $15^\circ$  for each bar) and this chart was transformed in a rose with the function `coord_polar()` of the package `ggplot2` (Wickham, 2016).

Lengths of trajectory segments ranged from 2.03 to 6.16 but were quite stable over time ( $3.46 \pm 1.06$ , total trajectory path = 69.14). At the end of the study period, distance to the initial state (5.79) was slightly higher than the mean value of net change ( $4.96 \pm 1.28$ ). Fig. 5 shows the ordination diagram representing the temporal variability of the community with respect to the initial state during the 21 years of sampling.

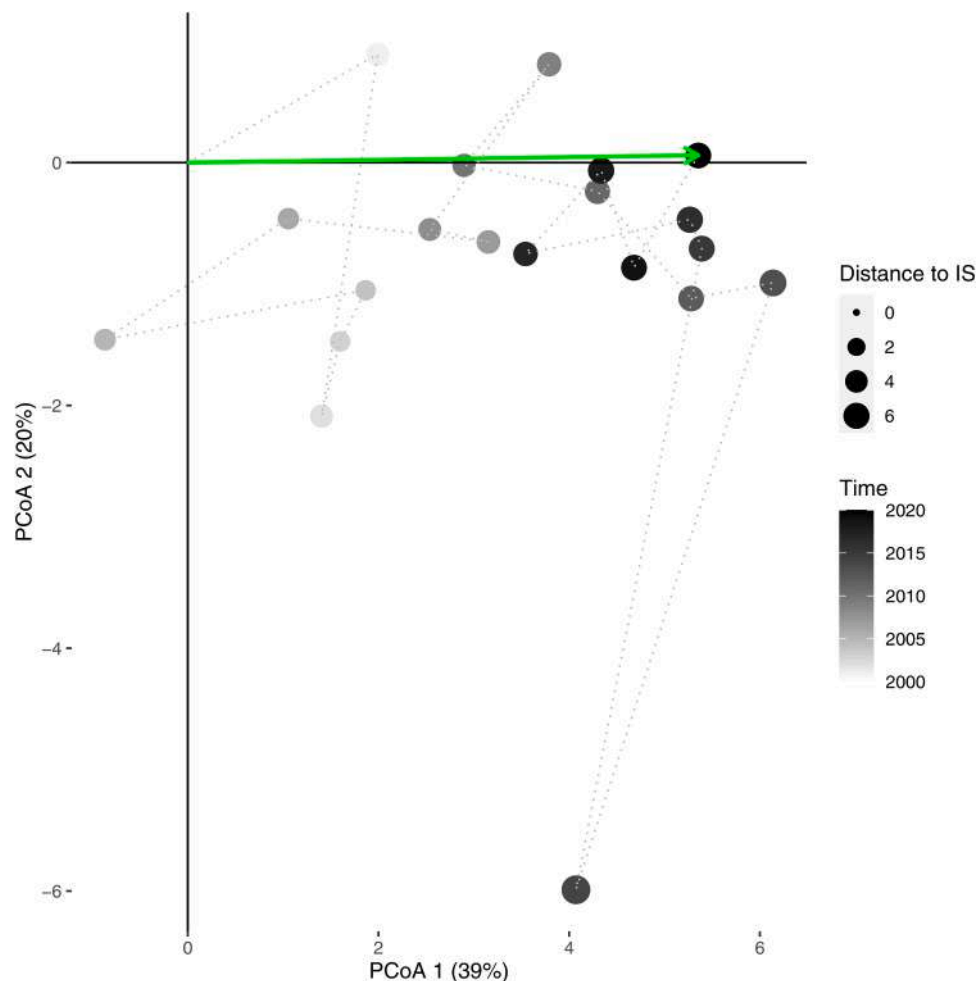


**Fig. 5.** Anatidae community state relative to the initial state chart between 1999 and 2020. The origin of the chart represents the initial state characterized in 1999, points represent intermediate ecological states [size=length of each state to initial state, colour= light grey (2000) to black (2020)] and lines represents segments between transitional state. The green arrow represents the net change between 2000 and 2020.

The first axis explained twice as much variance (39%) as the second axis (20%). Different species have influenced the anatidae community (Supplementary data – Appendix A). Three species mainly contribute to the first axis and are characterized by a clear decrease in numbers: *Branta bernicla*, *Mareca penelope*, and to a lesser extent *Mareca strepera*. Other species characterised by stable abundances or drastic interannual variations were mostly expressed on the second axis. The first axis highlights the temporal pattern of the community which is confirmed by the clustering of the most recent sampling occasions on the positive side of the first axis (Fig. 5).

The dominance of  $90^\circ < \Theta < 270^\circ$  (84.2%) and RIS and DIS alternation (Figs. 5 and 6, Supplementary data – Appendix A) suggest an ecological turnover in the species involved in ecological change. This results in a strong spring effect around the first state of each consecutive survey, which explains the very small NCR between 2000 and 2020 (8.35%) and low directionality (0.375). In absence of straight departing ( $0^\circ$ ) and recovering ( $180^\circ$ ) clear dominance, trajectory trends step by step to a different ecological state from 2000 to 2020.

The anatidae community mainly varied depending on the decline of two of the most numerous species *B. bernicla* and *Mareca penelope*. Other influencing species are not consistent over time which resulted in a clear spring effect around the initial state. CTA results confirmed conclusions of (Sturbois and Ponsero, 2019) and bring new insights concerning the way that ecological variability could be expressed through trajectory properties of bird communities within a given site.

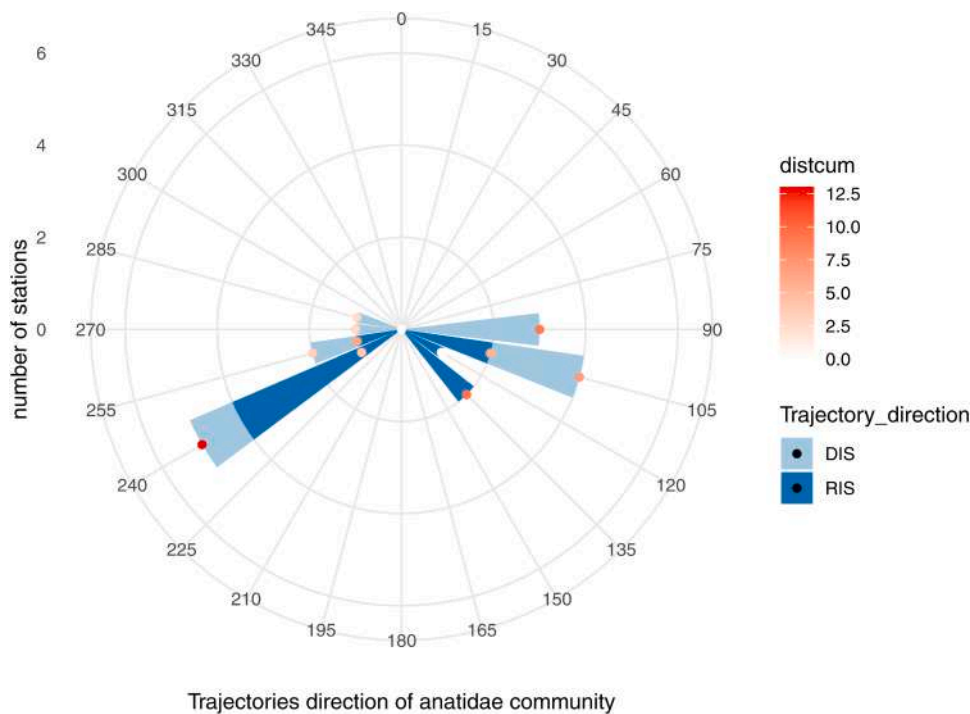


**Fig. 6.**  $\Theta$  trajectory rose for anatidae communities. Bars represent the number of segments concerned by each range ( $15^\circ$ ) of direction (RIS: dark blue; DIS: light blue). The length of the second segment of each triplet is represented with point at the head of each bar and coloured according to lengths values. Direction  $0^\circ$  represents a straight departing in the same direction as the first segment of each triplet. Direction  $180^\circ$  represents the direction of the return to the initial state (first ecological state of each triplet).

**3.2. Ecological application 2- Spatio-temporal changes of benthic communities in a modified system controlled for a tidal power station**

The spatio-temporal variability of benthic communities was studied

in the Rance estuary (Brittany, France), a modified system whose main physical characteristics are controlled by the functioning of a tidal power station (Desroy and Retière, 2004). The construction of the facility began in 1963 and was completed in 1966. Before the building of

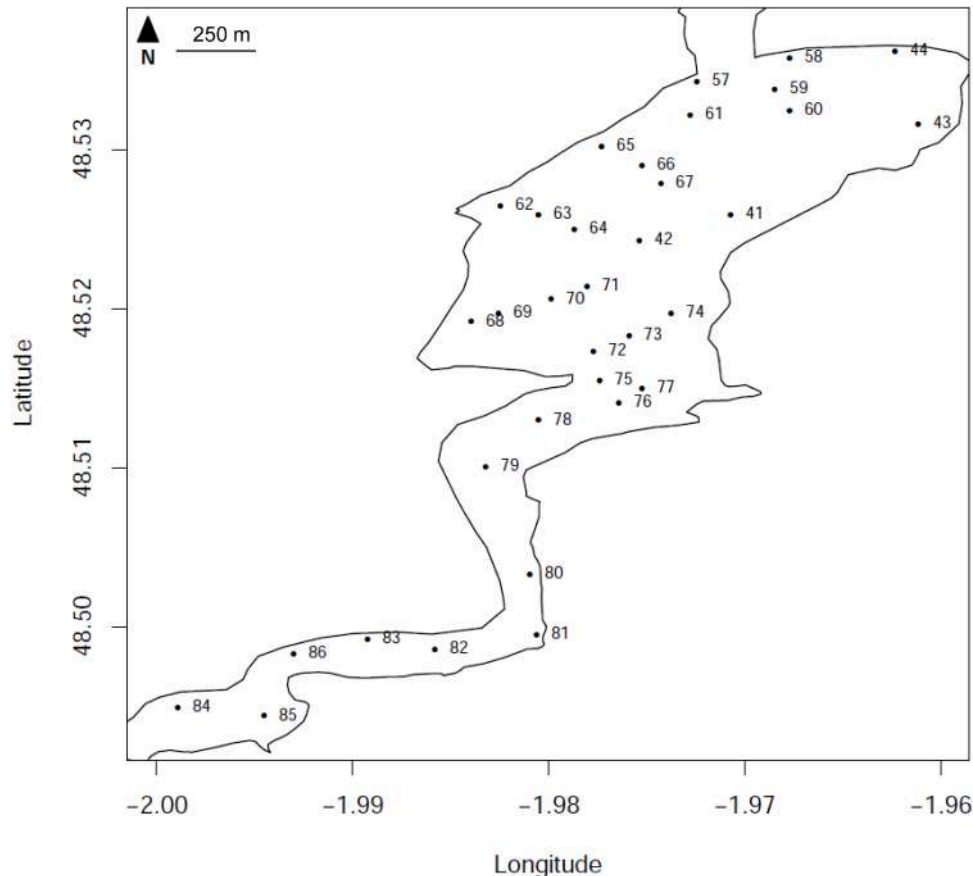


**Fig. 7.** Localisation of stations sampled in 1976, 1995 and 2010 in the upstream Rance, Brittany, France.

this infrastructure, the Rance was a ria with sectors differentiated by saline stratification whereas the system is now clearly separated into two main entities: the marine reservoir and the upstream estuary (brackish water). The construction step led to the formation of a hypohaline basin, inducing immediate strong mortality events for benthic macrofauna, and a period of instability (1967–1975). The control of the physical characteristics of the system has affected sediment dynamics, and deeply modified benthic habitats (Bonnot-Courtois, 1997; Bonnot-Courtois and Lafond, 1991; Retière, 1979).

Soft bottom benthic communities were sampled at 34 stations in 1976, 1995 and 2010 in the upstream estuary in order to analyse the ecological variability associated with the recovery process and sedimentary changes [Fig. 7, (Desroy and Retière, 2004)]. Temporal Beta-diversity Index [TBI (Legendre, 2019)] was run in order to verify if species gains or losses were responsible for net changes at the scale of both consecutive periods. A Hellinger transformation was performed on the overall data set prior to multivariate analysis (PCA) and coordinates of sites on the ordination diagram for the three surveys were used as inputs for community trajectory analysis (Supplementary data - Appendix C). A trajectory map was produced in order to synthesize trajectories of benthic communities on each site through the three surveys. After data aggregation depending on the station location (upstream vs down-stream), a second CTA analysis was performed in order to verify if local changes resulted in larger scale variations.

The species richness dramatically decreased from 149 species in 1976 to 54 and 73 species in 1995 and 2010, respectively. 27 species were common to the three surveys. A high variability of faunal composition was observed since 14 species appeared and 70 disappeared between 1976 and 1995 vs 38 new species and 19 less between 1995 and

2010. At the scale of the overall monitoring period, 34 new species were observed between 1976 and 2010 and 71 species disappeared. TBI index (0.46) confirms that species losses dominated species gains between 1976 and 1995 (losses for 18 stations and gains for 16 stations). Inversely gains dominated losses (0.60) for the 1995–2010 period (losses for 10 stations vs gains for 24 stations).

According to the cumulative trajectory path length of all sites, the first period was characterized by a higher ecological variability 539.69 ( $15.87 \pm 7.70$ ) than the second 469.92 ( $13.82 \pm 5.14$ ). Considering trajectory path length at the station scale, seven stations (59, 66, 63, 67, 57, 61, 58) represented 32.48% (327.96) of the whole trajectory path and segment lengths were more important during the second period for 13 stations (31,71%). Two main spatial trajectory patterns were identified (Fig. 8). Eight stations mainly located in the upstream part (south) of the study area were characterized by lower net ( $19.67 \pm 3.84$ ) and consecutive changes ( $9.07 \pm 2.30$ ). Inversely, higher changes characterized other stations mainly located in the downstream part (north), both at the scale of the overall study period ( $37.60 \pm 13.98$ ) and consecutive ones ( $16.41 \pm 6.43$ ). This increasing change along the upstream/downstream gradient is confirmed by significant correlations between latitude and net changes (0.40; p-value = 0.01944) and trajectory path lengths (0.45; p-value = 0.00685). RDT was positive for 12 sites and negative for 22, showing an overall departure dynamic from the initial state for 64.71% of sites, mainly located in the northern part of the study area (Fig. 8). Lower NCR values indicate significant direction changes between 1976 and 1995 and 1995–2010 trajectory segments (Supplementary data - Appendix C). It implies that changes are induced by different species groups between both periods. Differences in the magnitude of changes revealed at local scales areas also result in

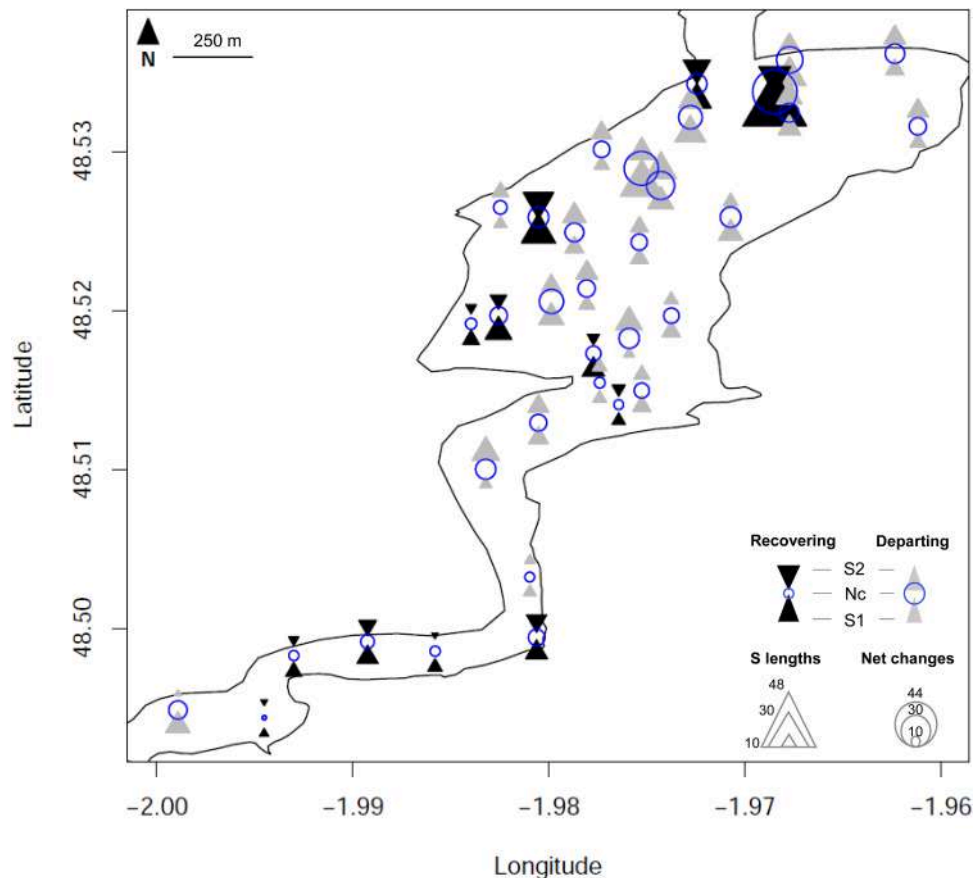


Fig. 8. Benthic community trajectory map. Net changes (Nc) are represented with blue circles between 1976 and 2010. Bottom triangles represent S1 (1976 to 1995) and top ones S2 (1995 to 2010). The size of the symbols corresponds to lengths. For triangles, colors are used to distinguish recovering (black) from departing trajectories (grey).

contrasted overall trends (Net change) at the larger scale of upstream (23.59) and downstream (49.77) communities.

The community described in 1976 was already undergoing a recovery process, which explains species losses and gains in the following surveys. According to the trajectory length of both periods and departing trajectories occurring in 64.71% of the stations, benthic communities are not yet stabilized in the study area. This seems particularly true for downstream stations which suffered most changes. In this area, regular changes in environmental conditions according to the estuary functioning influenced by the power station would probably not lead to a stabilization of benthic communities except if some species characterized by high dynamics induce long term changes of sediment facies (e.g. invasive species such as *Crepidula fornicata* and *Ruditapes philippinarum*). Future surveys will help to verify these hypotheses. Inversely, upstream stations are more stable probably due to environmental factors (influence of fresh water) which limit the variability of communities through a drastic selection of species.

### 3.3. Ecological application 3 – Temporal sedimentary variability in a marine intertidal area

Sediment facies were studied at 42 sites in the intertidal area of the bay of Saint-Brieuc in 1987 (Gros and Hamon, 1988), 2001 (Bonnot-Courtois and Dreau, 2002) and 2019 (Sturbois et al., unpublished data). At these dates, one sample of sediment was collected with a handcorer (5 cm diameter, depth of 5 cm) on each site and subsequently analysed for grain size distribution in the laboratory. Statistical analyses were performed with the package G2sd (Fournier et al., 2014). Sedimentary data from the three periods were combined in the same dataset subjected to CTA analysis (Supplementary data - Appendix D and E). Two TR were then produced in order to illustrate the distribution of  $\alpha$  angles for both periods with respect to sedimentary variables localised at the periphery of TR according to their position in the variable factor map (PCA). Finally, HR and Watson-William's tests were performed to test the homogeneity of angles distribution and the difference of segment direction between periods, respectively.

The first two dimensions of the PCA explained 81.8% of the variance so consideration of trajectory and segment properties with respect to these components is allowable. Trajectory path was lower for the period 1987–2001 (72.17;  $1.72 \pm 1.55$ ) than for the period 2001–2019 (99.67;  $2.37 \pm 1.96$ ) which indicated more sedimentary variability in the second period. However the sedimentary dynamics (i.e. speed of changes) was quantitatively quite similar for the two periods (1987–2001: 5.16 vs 2001–2019: 5.53). During the first period, 7 stations contributed to 46.38% of the trajectory path, whereas 12 stations were responsible for 59.20% of changes between 2001 and 2019 (Fig. 9, Supplementary data - Appendix D and E). This reveals that few sites are characterized by a

high sedimentary variability (length >3) while changes in most stations were more moderate. The TR qualitatively represents the pattern of the segments direction according to sedimentary variables (Fig. 10). During the first period, segment direction mainly occurred in the bottom part of the rose (HR test:  $T = 11.07$ , p-value=0.004) according to different sand variables from very fine to fine whereas for the segments of the second period it occurred in the top part of the rose (HR test:  $T = 13.77$ , p-value=0.002) according to very fine sand, mud and coarse sediment variables (Watson test:  $T = 0.896$ ; p-value<0.001). These results are consistent with the conclusions of Sturbois et al. (unpublished data) who showed that thirty years sedimentary changes in the intertidal part of the bay of Saint-Brieuc resulted in: (1) an overall slight sloughing revealed by the increase in the contribution of very fine sediment classes over the study period, (2) a high variability at few stations contrasting with moderate changes in the rest of the study area. This ecological application confirmed that angles and lengths are relevant trajectory properties to qualitatively and quantitatively describe trajectory patterns according to period or other factors such as habitat, management or pressure.

### 3.4. Ecological application 4 – Response of boreal forests to insect outbreaks

The spruce budworm (*Choristoneura fumiferana* Clem.) is considered amongst the most severe defoliating insects of boreal and sub-boreal forests of eastern North America (Blais, 1957). Every 30 to 40 years, its populations synchronously reaches outbreak levels over large spatial scales, generating dramatic ecological and economic impacts due to important mortality events in areas dominated by balsam fir (*Abies balsamea* L.) and spruce (*Picea* spp.). Whereas balsam fir usually presents higher levels of defoliation and mortality rates than spruce species of northern latitudes, a recent study (Sánchez-Pinillos et al., 2019) found a higher resilience of forests dominated by balsam fir than by black spruce (*P. mariana* Mill.). On the contrary, black spruce forests proved to be highly resistant to the insect attack but collapsed under long and severe outbreaks. We used a subset of plots affected by spruce budworm outbreaks and selected by Sánchez-Pinillos et al. (2019) from Quebec's Forest Inventory (Ministère des Ressources Naturelles, 2013) to assess forest responses to insect outbreaks with respect to individual pathways. In particular, we compared the dynamics of 74 mixed communities co-dominated by balsam fir and white birch (*Betula papyrifera* Marsh.) and 74 stands dominated by black spruce (Fig. 11). Forest plots were characterised with species abundance and size classes for the most common species. CTA metrics (Supplementary data - Appendix F) were used to characterize forest responses to the perturbation and a trajectory map was used to illustrate spatial patterns of trajectories according to the three types of responses to the outbreak (Sánchez-Pinillos et al.,

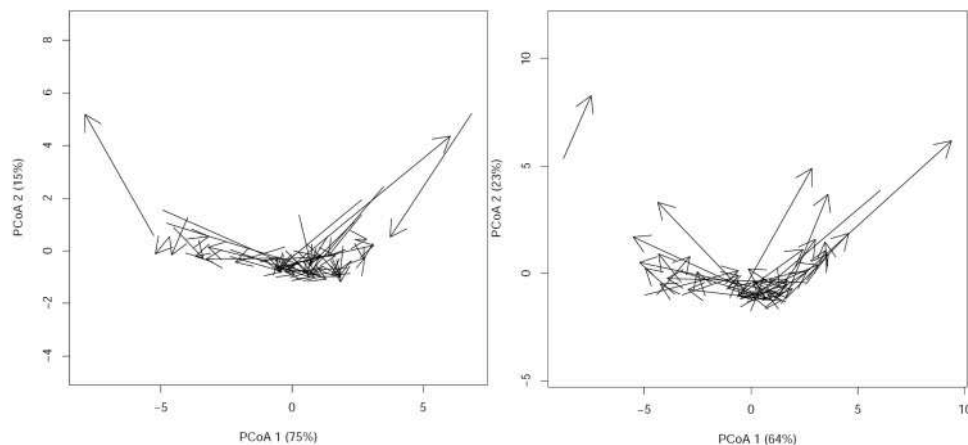


Fig. 9. Sedimentary trajectory segments. Arrows represents respectively 1987–2001 (left) and 2001–2019 (right) trajectory segments.

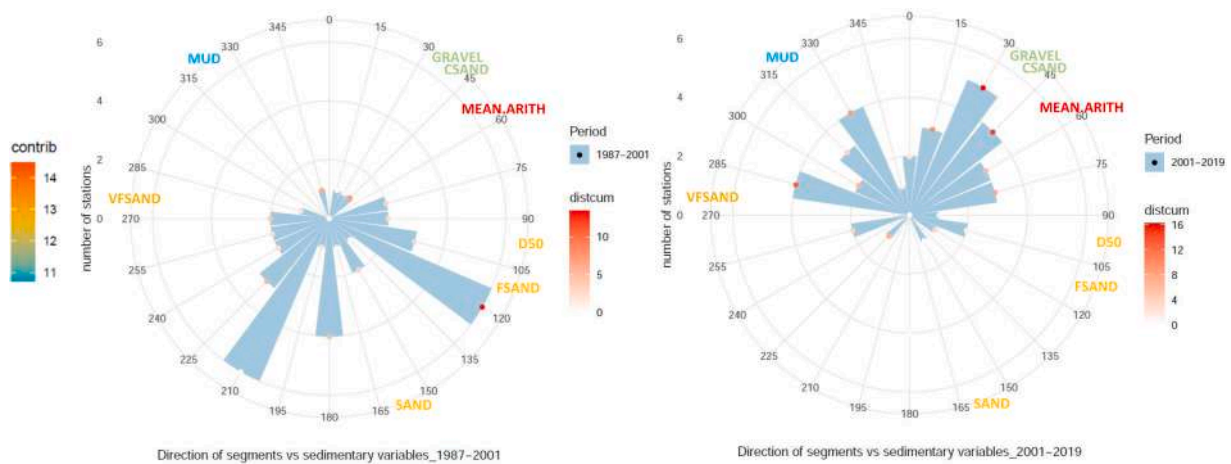


Fig. 10.  $\alpha$  trajectory roses for both periods (1987–2001 and 2001–2019) with respect to the two first components of the PCA (81.8% of the variance). Bars represent the number of stations concerned by each range (15°) of direction. Cumulative segment lengths are represented with point at the head of each bar and coloured according to length values. Sedimentary variables occurred in the periphery of the TR faithfully to the PCA ordination diagram and are coloured depending on their contribution to the two first component.

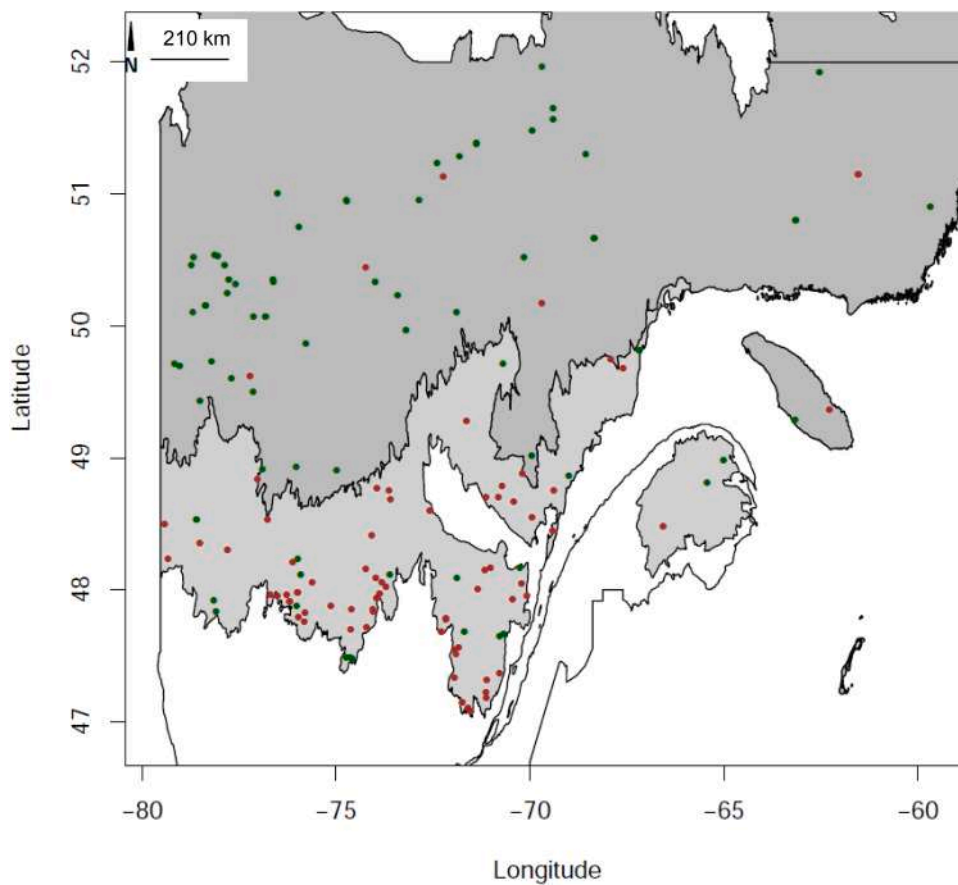


Fig. 11. Forest plots sampled in Quebec, Canada. Boreal zone dominated by Basalm fir - White birch appears in dark grey whereas zone dominated by Black spruce – Moss appears in light grey. Coloured dots indicates the type of forest on each station before the outbreak (pre-disturbance state): *ABBA-BEPA* in red and *PIMAhigh* in green.

2019). We finally used a TR of  $\omega$  distribution to illustrate differential responses according to the type of forest.

The changes of mixed fir-birch forests was reflected through longer trajectory paths (64.73) and lower net change (42.17) than the homologous in black spruce forests (47.70 and 59.95, respectively). However, both forests showed similar trajectory patterns, with longer distances

between the pre-disturbance and disturbed states (sum  $S_{1, fir-birch} = 37.95$ ; sum  $S_{1, spruce} = 39.12$ ) than between the disturbed and post-disturbance states (sum  $S_{2, fir} = 26.77$ ; sum  $S_{2, spruce} = 20.83$ ).

The trajectory map (Fig. 12) underlines the different responses of forests to the outbreak: (1) resistant plots were mainly characterized by departing dynamics and low segment length and net change, (2) resilient

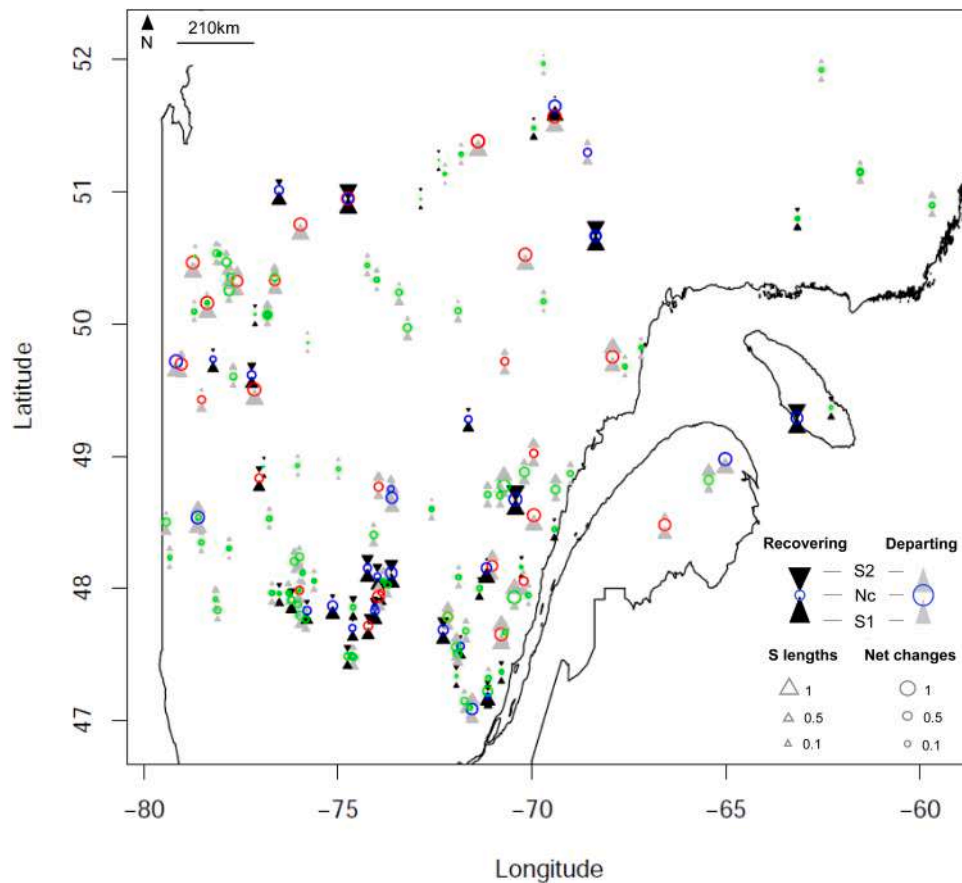


**Fig. 12.** Map of forest trajectories in response to insect outbreak. Net changes are represented by circles coloured according to forest responses to outbreak [resistant (green), resilient (blue) and changed (red)]. Bottom triangles represent S1 (pre-disturbance to disturbed state) and top ones S2 (disturbed to final state). Colours of triangles are used to distinguish recovering (black) from diverging trajectories (grey). The size of the symbols corresponds to lengths.

plots mainly occurred through recovering dynamics, high segment lengths, and moderate net change and, (3) changed plots were defined by departing dynamics and high segments lengths and net changes. In agreement with Sánchez-Pinillos et al. (2019), a higher percentage of recovering trajectories was found at southern latitudes, where balsam fir co-dominates the stands with white birch. Thus 42% of the plots classified as fir-white mixed forests showed recovering trajectories in comparison to the 30.1% of black spruce stands. On the contrary, shorter

trajectories were found above latitude 49°, reflecting the greater resistance of black spruce to the spruce budworm attack. It is important to note that, whereas we represented forest dynamics of all forest types in the same map, one could be interested in assessing the spatial differences in the responses of a given forest community. In such a case, a potential alternative could be to generate independent maps or different symbols or colours for each forest type.

TR diagrams of  $\omega$  distribution showed a clear rupture in trajectory

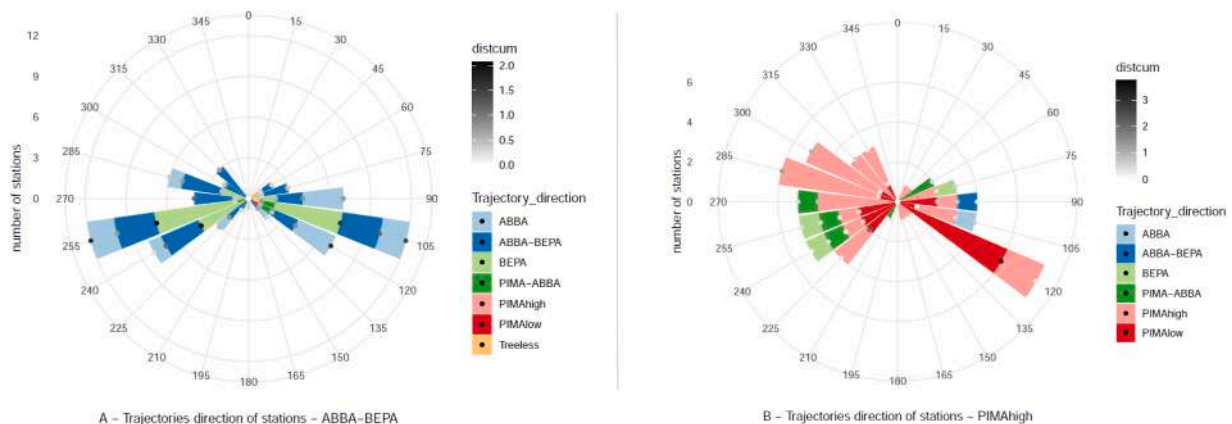


**Fig. 13.**  $\omega$  trajectory roses for forest plot characterised as ABBA-BEPA (A) or PIMAhigh (B) at the pre-disturbance state. Bars represent the number of segments concerned by each range (15°) of direction with coloured sections according to the type of forest defined at the final state. Cumulative lengths of the second segments (disturbed to final state) of each triplet are represented with point at the head of each bar and coloured according to lengths values (white to black). Direction 0° represents a straight departing in the same direction as the first segment of each triplet. Direction 180° represents the direction of the return to the initial state (first ecological state of each triplet).

direction between disturbed and final state for both forest typologies. Many plots did not show changes in forest classification. It is important to note that dissimilarities between forest surveys were calculated by considering different size classes for the most common species in boreal forests (*P. mariana*, *P. glauca*, *A. balsamea*, and *B. papyrifera*). The TR analyses, therefore, illustrated the changes in forest structure resulting from the death of the most vulnerable trees. Thus, most black spruce forests remained with the same composition after the outbreak or changed toward forests with a lower basal area represented by a different forest typology (Fig. 13-B, *PIMAhigh*). In the case of mixed forests of balsam fir and white birch (Fig. 13-A, *ABBA-BEPA*), our results showed different successional stages including the dominance of white birch colonizing gaps, a transient stage of mixed fir-birch stands, and a last successional stage dominated by balsam fir.

#### 4. Discussion

The CTA framework represents a valuable approach to assess ecological dynamics based on the geometric analysis of trajectories defined in a multidimensional space of community resemblance: geometric properties of trajectories, projection of a community state onto a trajectory, convergence/divergence and geometric resemblance between a pair of trajectories, spatial variation in community dynamics (De Cáceres et al., 2019).

Here, we went further in the definition of geometric properties of trajectories by complementing the available metrics and proposing synthetic methods of applied representation that facilitate the interpretation of ecosystem dynamics over time. For that, we integrated new tools (options, and new functions) into the original version of the CTA framework (available in package ‘vegclust’ on CRAN and GitHub repositories).

##### 4.1. Extending CTA metrics

The proposed extension makes the CTA framework more complete in order to address a larger panel of ecological questions, especially in applied ecology. The new metrics can be useful, for instance, when monitoring ecosystem responses to disturbances, or in the context of ecosystem restoration, by focusing CTA on geometric properties with respect to baseline ecological states. Net changes, new angles and the RDT metrics, along with recovering and departing characterisation of trajectories, allow addressing these issues, as shown in the case studies section.

The extension includes a new set of functions, based on the two first axes of the dissimilarity space in which trajectories were originally defined. This facilitates the use of CTA to users aiming to restrict analyses to a 2D Cartesian space or to study trajectories in a biplot including only two variables. As the first two axes often explain a part of the total variance, the user must be cautious with the interpretation of the angles used in trajectory roses, particularly when the two first axes explain a small proportion of total variance. When most variance proportion is captured, we consider that these metrics can be compared to variables in multivariate spaces in order to provide ecological meaning to the direction. When using  $\Theta$  and  $\omega$  angles in TR, CTA returns angles between trajectory segments regarding 2D point coordinates of the third survey of each triplet with respect to the previous segment. The variance explained by the first two axis remains also important here to evaluate the relevance of angles transformations even if the coordinates of the third point in the 2D space are only used to flip the 0–180 angles in positive or negative. Consequently, this step does not influence the accuracy of angle calculations considering all components. As each triplet forms its own plane it is not possible to provide an ecological meaning related to the environmental variables, but we consider that this step of the procedure still contributes to efficiently illustrating the degree of ecological variability.

As shown in the second case study, CTA allows the comparison of

cumulative (departing) or buffering (recovering) local trajectory patterns with changes at higher community levels in the multivariate space. Measuring changes at these two scales, local vs assemblage or community, help to determine if small scale changes result in larger scale variations. It helps for the potential detection of 1. station dispersion occurring without significant centroid variations at community scale, or 2. cyclic community variability contrasting with constant departing trajectories in other community.

Further CTA extensions could be envisaged, beyond the one presented here. To complete the qualitative characterisation of recovering and departing trajectories, an interesting potential extension of CTA may concern the routine definition of trajectory shape with respect to the occurrence of saltatory and non-directional trajectories (Lamothe et al., 2019; Matthews et al., 2013). Another perspective of CTA extension could concern the integration of figures codes (Supplementary data - Appendix G) in graphical functions in order to produce trajectory maps, charts, and roses.

##### 4.2. Representing trajectory properties

We presented and illustrated set of innovative figures to represent trajectory properties, offering an interesting alternative to traditional representations used in community ecology and other fields where temporal series are naturally multivariate.

###### 4.2.1. Maps of trajectory properties

Mapping trajectory properties allows the illustration of spatio-temporal patterns taking into account all the variability contained in multivariate analysis. Information about net change and dynamics occurring within the whole study period at a site level is consequently efficiently synthesized and sites characterized by stability or high ecological variability are easily identifiable. The forest application (Section 3.4) highlighted the ability of trajectory maps to illustrate the potential link between CTA metrics and other indices. In this article, we used lengths, trajectory path and net change as inputs to map RIS and DIS dynamics. We encourage also users to represent other CTA metrics (e.g. overall trajectory length or speed, directionality or NCR) or the behaviour over time of diversity indices or any other ecological variables coming from other analytical frameworks.

###### 4.2.2. Adding CTA metrics to ordination diagrams

An ordination diagram centred on the initial state of a trajectory allows highlighting both the whole shape of the trajectory (i.e. lengths and angles) and the distance to the baseline state (i.e. the net change) at each survey of the study period. In ecological application 3.1, net changes include all n-dimensional components, but coordinates of data points and lines originate from 2D representation of trajectories. If the first two multivariate axes do not explain a sufficient part of the variance, the representation of the distance to the initial state should not be optimal for trajectory path which is the best fit with other components. If one should prioritize between the representations of distances to initial states for the relative trajectory directions, a good approach would be to centre trajectories considered individually. In this way, each trajectory path could express itself on the 2D graph with its maximal variability. When the first two axes of multivariate analyses explain the main part of the variance, the first option fulfills correctly both the distance and relative direction considerations.

In case of ecological cycles, the net changes, as well as directionality, are two good metrics to illustrate distancing trajectories following by recovering patterns. The relative to initial state chart proposed in Section 2.2.2 and Fig. 5, or a simple 2D graph representing net changes according to time could be useful to represent alternative distancing and recovering trajectories inherent to ecological cycle. However, long time series are needed to be able to describe ecological cycles.

#### 4.2.3. Using trajectory roses and circular statistics together with CTA

The trajectory rose concept offers an innovative way to represent angles and lengths at the scale of a study area with the possibility to explain metrics by explanatory variables using the bar sections of the TR (RIS or DIS trajectories, period, habitat, pressure, management...). Doing this, the TR allows visualization of direction trend changes with corresponding lengths and offers a synthetic way to illustrate ecological variability in response to natural or anthropogenic factors. The different variants of the TR diagrams, related to different types of angles, are useful in representing the distribution of temporal changes in the direction of community or ecosystem dynamics and circular statistics allows testing and comparing these patterns. Used together, CTA metrics and circular statistics are helpful to quantitatively analyse trajectories and compare directions, since they provide important insights into elements of community or ecosystem dynamics that are not evident from qualitative descriptions of multivariate ordination diagrams.

#### 4.3. Applications and limitations of the proposed framework

Multivariate ecological methods are descriptive by nature. Despite CTA allows more precise measurement and illustration of ecological changes, it suffers the same limitations. Consequently, users should complete CTA outputs by a strong specific examination of datasets (i.e. species or other variables) in order to improve the ecological meaning of observed changes, as done in the four ecological applications of this paper, or by complementing CTA with additional analyses providing statistical background on community changes. Otherwise, conclusions provide an incomplete picture and can mislead the description of ecological states (Cimon and Cusson, 2018) with potential misdirecting conservation actions or overstating conservation progress.

Note that ordination spaces are specifically constructed for each given data set. Therefore, any data transformation on the raw data or sampling decision is likely to affect trajectories, and subsequently, all metrics to be calculated. We alert future users and urge them to test for this effect before any overall transformations, change in sampling design and/or suppression of rare species in a community data set. Furthermore, when choosing a dissimilarity coefficient, users should check the properties the coefficient has, to determine whether they are suitable for the objectives of the study (Legendre and De Cáceres, 2013) and implications in CTA performing.

Users should also be aware of the importance of the definition of the first state of a time series. If a sampling program starts in the middle of a disturbing event it will not be possible to measure the overall ecological response to disturbance because sampling design prevents the definition of a predisturbance state. This “missing part” of the ecological trajectory depends on sampling starting according to disturbing events and the type of disturbance. In applications characterized by cyclic variability, the ecological cycle will be underlined whatever the first survey used to identify the first ecological state of the time series. However, the position of this first state within the ecological cycle would only be identified regarding future surveys.

Despite the CTA framework has no limit on the number of components considered in metric calculations, some of new applications (reporting angles  $\Theta$ ,  $\omega$  in a 0–360° system, angle  $\alpha$  calculation) refer to the first two components. In this context, performing CTA analysis imposes a careful interpretation of the multivariate space in order to assess the consequences of such environment reduction. Consequently, users have to assume and decide if the variance explained is sufficient to calculate these CTA metrics.

#### 4.4. CTA as a useful multivariate toolbox

Whereas the extended CTA framework and the associated modes of representation constitute potential management and decision-making tools, we urge users interested in sharing our synthetic tools with managers or stakeholders that interpretation must be done carefully

with a hand of experienced multivariate ecologists and necessarily coupled with a precise data examination. In restoration or perturbation contexts, lengths, net change, and RDT metrics allow a real-time measurement (i.e. after each survey) of ecological dynamics in response to management interventions or potential disturbances, and a quantitative assessment of the degree of success in achieving conservation objectives or the impact of natural or anthropogenic changes on environmental conditions. In this perspective, consideration of angles is complementary to length-based approaches and allows, for instance, the identification of changes in variables responsible for ecological changes (as in TR based on  $\Theta$  angles), as well as the interpretation of the nature of these changes (TR based on  $\alpha$  angles).

Our extended CTA framework and our new representation tools can easily be applied to other input data and fields in ecology (e.g. abundance, biomass, biometry, functional traits, food web) and beyond, as it is illustrated in the four case studies. This framework provides useful tools in order to (1) assess the achievement of restoration goal (recovering after perturbation), (2) highlight ecosystem modifications (departing to the initial state), (3) highlight different ecosystem responses regarding chosen factors (RDT and angles), and (4) to potentially contribute to the documentation and the representation of long-term monitoring observatories.

In conclusion, the CTA metrics and the extension provide a valuable toolbox for trained ecologists (aware of multivariate applications and limitations), to analyse ecological variability and trajectories with respect to a baseline state. The case studies highlighted the complementarity and the ability of our figure concepts to illustrate spatio-temporal trends of different fields in ecology and to modestly contribute to the facilitation of their interpretation.

#### Declaration of Competing Interest

The authors declare that they have no known competing financial interests or personal relationships that could have appeared to influence the work reported in this paper.

#### Acknowledgments

We acknowledge Agence de l'eau Loire-Bretagne (grant number 180212501), Région Bretagne (grant number OSIRIS PFEA621219CR0530023), Europe for the European maritime and fisheries fund (grant number FEAMP 621-B) and Ministère de la transition écologique et solidaire (grant number EJ N°2102930123) who funded this research as part of the ResTroph Baie de Saint-Brieuc research program. We thank anonymous reviewers of previous versions of this manuscript for their constructive comments. We acknowledge Geoffrey and Alexander Stevens for English text improvement and Pascal Riera for proofreading.

#### Supplementary materials

Supplementary material associated with this article can be found, in the online version, at [doi:10.1016/j.ecolmodel.2020.109400](https://doi.org/10.1016/j.ecolmodel.2020.109400).

#### References

- Austin, M.P., 1977. Use of ordination and other multivariate descriptive methods to study succession. *Vegetatio* 35, 165–175. <https://doi.org/10.1007/BF02097067>.
- Azorin-Molina, C., Vicente-Serrano, S.M., McVicar, T.R., Revuelto, J., Jerez, S., López-Moreno, J.-I., 2017. Assessing the impact of measurement time interval when calculating wind speed means and trends under the stilling phenomenon: Impact of measurement time interval on wind speed means and trends. *Int. J. Climatol.* 37, 480–492. <https://doi.org/10.1002/joc.4720>.
- Bacouillard, L., Baux, N., Dauvin, J.-C., Desroy, N., Geiger, K.J., Gentil, F., Thiébaud, É., 2020. Long-term spatio-temporal changes of the muddy fine sand benthic community of the Bay of Seine (eastern English Channel). *Mar. Environ. Res.* 161, 105062 <https://doi.org/10.1016/j.marenvres.2020.105062>.
- Bagchi, S., Singh, N.J., Briske, D.D., Bestelmeyer, B.T., McClaran, M.P., Murthy, K., 2017. Quantifying long-term plant community dynamics with movement models:

- implications for ecological resilience. *Ecol. Appl.* 27, 1514–1528. <https://doi.org/10.1002/eap.1544>.
- Batschelet, E., 1981. *Circular Statistics in Biology*. Academic Press, NY, 111 FIFTH AVE N. Y. 10003 1981 388.
- Bioret, F., Estève, R., Sturbois, A., 2009. Dictionnaire De La Protection De La Nature 1. Blais, J.R., 1957. Some relationships of the spruce budworm, *Choristoneura fumiferana* (Clem.) to black spruce, *Picea mariana* (Moench) Voss. *For. Chron.* 33, 364–372.
- Boit, A., Spencer, M., 2019. Equivalence and dissimilarity of ecosystem states. *Ecol. Model.* 396, 12–22. <https://doi.org/10.1016/j.ecolmodel.2019.01.009>.
- Bonnot-Courtois, C., 1997. Evolution de la répartition des sédiments dans l'estuaire de la Rance, 1883-1994. Atlas permanent de la mer et du littoral. CNRS, Géolittomer, UMR6554, Editmar.
- Bonnot-Courtois, C., Dreau, A., 2002. Cartographie Morpho-Sédimentaire De L'estran En Baie de Saint-Brieuc. Laboratoire de Géomorphologie et environnement littoral-DIREN Bretagne.
- Bonnot-Courtois, C., Lafond, L.R., 1991. Caractérisation et comportement des vases dans l'estuaire de la Rance. Rapport contrat Electricité de France.
- Buckley, H.L., Day, N.J., Case, B.S., Lear, G., Ellison, A.M., 2018. Multivariate methods for testing hypotheses of temporal community dynamics (preprint). *Ecology*. <https://doi.org/10.1101/362822>.
- Cieszynska, A., Stramska, M., 2018. Climate-related trends and meteorological conditions in the Porsanger fjord, Norway. *Oceanologia* 60, 344–366. <https://doi.org/10.1016/j.oceano.2018.01.003>.
- Cimon, S., Cusson, M., 2018. Impact of multiple disturbances and stress on the temporal trajectories and resilience of benthic intertidal communities. *Ecosphere* 9, e02467. <https://doi.org/10.1002/ecs2.2467>.
- Dalbosco, A.L.P., Franco, D., Barletta, R.do C., Trevisan, A.B., 2020. Analysis of currents on the continental shelf off the Santa Catarina Island through measured data. *RBRH* 25, e7. <https://doi.org/10.1590/2318-0331.252020180175>.
- Dauvin, J.-C., Ibanez, F., 1987. Variations à long-terme (1977-1985) du peuplement des sables fins de la Pierre Noire (baie de Morlaix, Manche occidentale): analyse statistique de révolution structural. In: Heip, C., Keegan, B.F., Lewis, J.R. (Eds.), *Long-Term Changes in Coastal Benthic Communities*. Springer Netherlands, Dordrecht, pp. 171–186. [https://doi.org/10.1007/978-94-009-4049-9\\_16](https://doi.org/10.1007/978-94-009-4049-9_16).
- David, V., Tortajada, S., Philippine, O., Bréret, M., Barnett, A., Agogue, H., Robin, F.-X., Dupuy, C., 2020. Ecological succession and resilience of plankton recovering from an acute disturbance in freshwater marshes. *Sci. Total Environ.* 709, 135997. <https://doi.org/10.1016/j.scitotenv.2019.135997>.
- De Cáceres, M., Coll, L., Legendre, P., Allen, R.B., Wiser, S.K., Fortin, M., Condit, R., Hubbell, S., 2019a. Trajectory analysis in community ecology. *Ecol. Monogr.* 89, e01350. <https://doi.org/10.1002/ecm.1350>.
- De Cáceres, M., Coll, L., Legendre, P., Allen, R.B., Wiser, S.K., Fortin, M., Condit, R., Hubbell, S., 2019b. Trajectory analysis in community ecology. *Ecol. Monogr.* 89, e01350. <https://doi.org/10.1002/ecm.1350>.
- Desroy, N., Retière, C., 2004a. Using benthos as a tool for coastal management: the impact of the tidal power station on benthic communities of the Rance basin. *Aquat. Ecosyst. Health Manag.* 7, 59–72. <https://doi.org/10.1080/14634980490281263>.
- Desroy, N., Retière, C., 2004b. Using benthos as a tool for coastal management: the impact of the tidal power station on benthic communities of the Rance basin. *Aquat. Ecosyst. Health Manag.* 7, 59–72. <https://doi.org/10.1080/14634980490281263>.
- Dornelas, M., Magurran, A.E., Buckland, S.T., Chao, A., Chazdon, R.L., Colwell, R.K., Curtis, T., Gaston, K.J., Gotelli, N.J., Koskin, M.A., McGill, B., McCune, J.L., Morlon, H., Mumby, P.J., Øvreås, L., Stuedeny, A., Vellend, M., 2013. Quantifying temporal change in biodiversity: challenges and opportunities. *Proc. R. Soc. B Biol. Sci.* 280, 20121931. <https://doi.org/10.1098/rspb.2012.1931>.
- Dufresne, C., Duffa, C., Rey, V., 2014. Wind-forced circulation model and water exchanged through the channel in the Bay of Toulon. *Ocean Dyn.* 64, 209–224. <https://doi.org/10.1007/s10236-013-0676-3>.
- Elton, C.S., 1927. In: Sidgwick, Jackson (Eds.). London.
- Fournier, J., Gallon, R.K., Paris, R., 2014. G2Sd: a new package for the statistical analysis of unconsolidated sediments. *Géomorphologie Relief Process. Environ.* 1, 73–78.
- Fukami, T., Martijn Bezemer, T., Mortimer, S.R., Putten, W.H., 2005. Species divergence and trait convergence in experimental plant community assembly. *Ecol. Lett.* 8, 1283–1290. <https://doi.org/10.1111/j.1461-0248.2005.00829.x>.
- Granger, V., Bez, N., Fromentin, J., Meynard, C., Jadaud, A., Mérigot, B., 2015. Mapping diversity indices: not a trivial issue. *Methods Ecol. Evol.* 6, 688–696. <https://doi.org/10.1111/2041-210X.12357>.
- Gros, P., Hamon, D., 1988. Typologie Biosédimentaire De La Baie de Saint-Brieuc (Manche ouest) Et Estimation De La Biomasse Des Catégories Trophiques Macrozoobenthiques. IFREMER.
- Haig, S.M., Murphy, S.P., Matthews, J.H., Arismendi, I., Safeeq, M., 2019. Climate-altered wetlands challenge waterbird use and migratory connectivity in arid landscapes. *Sci. Rep.* 9. <https://doi.org/10.1038/s41598-019-41135-y>.
- Hudson, A., Bouwman, H., 2007. Different land-use types affect bird communities in the Kalahari. *South Africa. Afr. J. Ecol.* 45, 423–430. <https://doi.org/10.1111/j.1365-2028.2006.00750.x>.
- Kendall, B.E., 2015. Some directions in ecological theory. *Ecology* 96, 3117–3125. <https://doi.org/10.1890/14-2080.1>.
- Kendall, M.G., 1958. A Course in Multivariate Analysis. By M. G. Kendall, Sc.D. (No. 2 in Griffin's Statistical Monographs and Courses.) [Pp. 185. London: Charles Griffin, 1957. 22]. *J. Inst. Actuar.* 84, 112–113. <https://doi.org/10.1017/S0020268100037422>.
- Kröncke, I., Reiss, H., Eggleton, J.D., Aldridge, J., Bergman, M.J.N., Cochrane, S., Craeymeersch, J.A., Degraer, S., Desroy, N., Dewarumez, J.-M., Duineveld, G.C.A., Essink, K., Hillewaert, H., Lavaleye, M.S.S., Moll, A., Nehring, S., Newell, R., Oug, E., Pohlmann, T., Rachor, E., Robertson, M., Rumohr, H., Schratzberger, M., Smith, R., Berghe, E.V., van Dalßen, J., van Hoey, G., Vincx, M., Willems, W., Rees, H.L., 2011. Changes in North Sea macrofauna communities and species distribution between 1986 and 2000. *Estuar. Coast. Shelf Sci.* 94, 1–15. <https://doi.org/10.1016/j.ecss.2011.04.008>.
- Lamothe, K.A., Somers, K.M., Jackson, D.A., 2019. Linking the ball-and-cup analogy and ordination trajectories to describe ecosystem stability, resistance, and resilience. *Ecosphere* 10, e02629. <https://doi.org/10.1002/ecs2.2629>.
- Landler, L., Ruxton, G.D., Malkemper, E.P., 2019. The Hermans-Rasson test as a powerful alternative to the Rayleigh test for circular statistics in biology. *BMC Ecol.* 19, 30. <https://doi.org/10.1186/s12898-019-0246-8>.
- Landler, L., Ruxton, G.D., Malkemper, E.P., 2018. Circular data in biology: advice for effectively implementing statistical procedures. *Behav. Ecol. Sociobiol.* 72, 128. <https://doi.org/10.1007/s00265-018-2538-y>.
- Legendre, P., 2019. A temporal beta-diversity index to identify sites that have changed in exceptional ways in space-time surveys. *Ecol. Evol.* 9, 3500–3514. <https://doi.org/10.1002/ece3.4984>.
- Legendre, P., De Cáceres, M., 2013. Beta diversity as the variance of community data: dissimilarity coefficients and partitioning. *Ecol. Lett.* 16, 951–963. <https://doi.org/10.1111/ele.12141>.
- Legendre, P., Gauthier, O., 2014. Statistical methods for temporal and space-time analysis of community composition data <sup>/>. *Proc. R. Soc. B Biol. Sci.* 281, 20132728. <https://doi.org/10.1098/rspb.2013.2728>.
- Legendre, P., Salvat, B., 2015. Thirty-year recovery of mollusc communities after nuclear experiments on Fangataufa atoll (Tuamotu, French Polynesia). *Proc. R. Soc. B Biol. Sci.* 282, 20150750. <https://doi.org/10.1098/rspb.2015.0750>.
- Magurran, A.E., Dornelas, M., Moyes, F., Henderson, P.A., 2019. Temporal  $\beta$  diversity—A macroecological perspective. *Glob. Ecol. Biogeogr.* 28, 1949–1960. <https://doi.org/10.1111/gcb.13026>.
- Mathers, K.L., Chadd, R.P., Dunbar, M.J., Extence, C.A., Reeds, J., Rice, S.P., Wood, P.J., 2016. The long-term effects of invasive signal crayfish (*Pacifastacus leniusculus*) on instream macroinvertebrate communities. *Sci. Total Environ.* 556, 207–218. <https://doi.org/10.1016/j.scitotenv.2016.01.215>.
- Matthews, W.J., Marsh-Matthews, E., Cashner, R.C., Gelwick, F., 2013. Disturbance and trajectory of change in a stream fish community over four decades. *Oecologia* 173, 955–969. <https://doi.org/10.1007/s00442-013-2646-3>.
- McLean, M., Mouillot, D., Lindegren, M., Villéger, S., Engelhard, G., Murgier, J., Auber, A., 2019. Fish communities diverge in species but converge in traits over three decades of warming. *Glob. Change Biol.* 25, 3972–3984. <https://doi.org/10.1111/gcb.14785>.
- Ministère des Ressources Naturelles, 2013. Données descriptives des placettes-échantillons permanentes.
- Retière, C., 1979. Contribution à La Connaissance Des Peuplements Benthiques Du Golfe Normano-Breton. Rennes I.
- Sánchez-Pinillos, M., Leduc, A., Ameztegui, A., Kneeshaw, D., Lloret, F., Coll, L., 2019. Resistance, resilience or change: post-disturbance dynamics of boreal forests after insect outbreaks. *Ecosystems* 22, 1886–1901. <https://doi.org/10.1007/s10021-019-00378-6>.
- Schmidt, S.N., Olden, J.D., Solomon, C.T., Zanden, M.J.V., 2007. Quantitative approaches to the analysis of stable isotope food web data. *Ecology* 88, 2793–2802. <https://doi.org/10.1890/07-0121.1>.
- Sica, Y.V., Gavier-Pizarro, G.I., Pidgeon, A.M., Travaini, A., Bustamante, J., Radeloff, V. C., Quintana, R.D., 2018. Changes in bird assemblages in a wetland ecosystem after 14 years of intensified cattle farming. *Austral Ecol.* 43, 786–797. <https://doi.org/10.1111/aec.12621>.
- Smith, J.E., Hunter, C.L., Smith, C.M., 2010. The effects of top-down versus bottom-up control on benthic coral reef community structure. *Oecologia* 163, 497–507. <https://doi.org/10.1007/s00442-009-1546-z>.
- Sturbois, A., Ponsoer, A., 2019. Evolution des populations de limicoles et d'anatidés en baie de Saint-Brieuc. *Ornithos* 26, 232–243.
- Wickham, H., 2016. *ggplot2, Use R!*. Springer International Publishing, Cham. <https://doi.org/10.1007/978-3-319-24277-4>.
- Yang, L.H., 2020. Toward a more temporally explicit framework for community ecology. *Ecol. Res.* 35, 445–462. <https://doi.org/10.1111/1440-1703.12099>.